ELSEVIER

Effect of noise on excursions to and back from infinity

Jeff Moehlis

Program in Applied and Computational Mathematics, Princeton University, Princeton, NJ 08544-1000, USA

Abstract

The effect of additive white noise on a model for bursting behavior in large aspect-ratio binary fluid convection is considered. Such bursts are present in systems with nearly square symmetry and are the result of heteroclinic cycles involving infinite amplitude states created when the square symmetry is broken. A combination of numerical results and analytical arguments shows how even a very small amount of noise can have a very large effect on the amplitudes of successive bursts. Large enough noise can also affect the physical manifestations of the bursts. Finally, it is shown that related bursts may occur when white noise is added to the normal form equations for the Hopf bifurcation with exact square symmetry. © 2001 Elsevier Science B.V. All rights reserved.

1. Introduction

In physical systems, noise is unavoidable. Thus, it is important to study the effect of noise on models of physical systems. It has been shown that some models are very sensitive to the presence of noise: for example, the model for the resonant interaction of three wave modes considered in [1–3] shows that a tiny amount of noise can replace a bifurcation structure involving a period doubling cascade to chaos with a noisy periodic orbit which is attracting over a wide range of parameter values. This may be understood in terms of the slow–fast character of the dynamics for this model. In the absence of noise, during the slow phase the trajectory moves near an invariant plane from a region where the plane is attracting to a re-

gion where it is repelling. The closer the trajectory gets to the invariant plane in the attracting region, the larger the subsequent fast excursion which reinjects the trajectory near the attracting region. The presence of noise perturbs the trajectory away from the invariant plane during the slow phase, thereby limiting the size of the fast excursions and effectively destroying the chaotic behavior. Related effects of noise occur for models of other systems with slow–fast behavior including pulsating laser oscillations [4] and the shear instability of tall convection cells [5]. Noise can also have a profound effect on models with structurally stable heteroclinic cycles. These cycles involve connections between unstable states, and the connections typically occur in invariant subspaces. Even small amounts of noise can cause the system to jump across these subspaces, and this can lead to very different dynamical behavior [6]. If such a heteroclinic cycle also is *attracting*, the time spent in the neighborhood of the

unstable states of the cycle increases without bound with increasing time. This is not observed in physical systems and noise provides an explanation: the heteroclinic cycle becomes a "statistical limit cycle" in which switching between the unstable states of the cycle occurs randomly in time but with a well-defined mean period [7–9]. Finally, we mention the phenomenon of stochastic resonance in which a weak periodic signal can be greatly enhanced by the presence of noise. Specifically, there is an optimal noise strength which gives a peak in the signal-to-noise ratio for the system. First proposed as a mechanism by which ice ages occur roughly periodically in time [10–12], stochastic resonance has since been observed in models and experiments for a large variety of physical and biological systems (see [13,14] and references therein).

In [15,16], a model of large aspect-ratio binary fluid convection was studied. The model considers the competition between two nearly degenerate modes of opposite parity. The evolution equations correspond to a Hopf bifurcation with broken D_4 symmetry, where the "interchange" symmetry between the two modes is weakly broken because of the large but finite aspect-ratio. For open parameter regimes, periodic or irregular bursting with very large dynamic range can occur close to threshold. The bursts are associated with nonattracting heteroclinic cycles involving solutions "at infinity" [16,17]. These cycles may be structurally stable or unstable. Bursts occur when the system evolves toward an infinite amplitude state along its stable manifold, then gets kicked toward another infinite amplitude state with an unstable manifold which returns the system to finite amplitude. This mechanism provides an explanation for bursts found experimentally for large aspect-ratio binary fluid convection [18], and may also provide a deterministic explanation for the variability of the solar magnetic cycle [19]. Related bursts can occur due to the resonant temporal forcing of a system undergoing a Hopf bifurcation with D_4 symmetry [20]. There are many other mechanisms that lead to behavior that has been described as "bursting" in hydrodynamical and neural systems; a review of such mechanisms is given in [21,22].

When noise is added to the model considered in [15, 16], there will be a burst with larger amplitude if the noise kicks the system closer to the stable manifold of an infinite amplitude state, and a burst with smaller amplitude if the noise kicks it away. Thus a state which

bursts in the absence of noise is still expected to burst in the presence of noise, but the successive burst amplitudes and the time between successive bursts may change substantially. The details of the effect of noise on the bursting behavior are described in this Letter. This includes the possibility that noise can affect the physical manifestations of the bursts. Specifically, purely blinking and winking states in which successive bursts occur at opposite sides or the same side of the container, respectively, can be destroyed by sufficiently large noise. Finally, it is shown that related bursts can occur even if the D_4 symmetry of the model is *not* broken, i.e., when noise is added to the normal form equations for the Hopf bifurcation with *exact* D_4 symmetry.

2. Evolution equations for the model

For binary fluid convection, if the separation ratio of the mixture is sufficiently negative then convection arises via a Hopf bifurcation. This is the case for the $^3He/^4He$ mixture used by Sullivan and Ahlers [18] in their experiment carried out in the large aspect-ratio rectangular container

$$
D \equiv \left\{ (X, Y, Z) \,\middle|\, -\frac{1}{2}\Gamma \leqslant X \leqslant \frac{1}{2}\Gamma, \right.
$$
$$
\left. -\frac{1}{2}\Gamma_Y \leqslant Y \leqslant \frac{1}{2}\Gamma_Y, \ -\frac{1}{2} \leqslant Z \leqslant \frac{1}{2} \right\},
$$

with aspect-ratio $\Gamma = 34$ and $\Gamma_Y = 6.9$. In this experiment, it was observed that immediately above threshold convective heat transport may take place in a sequence of irregular bursts of large dynamic range despite constant heat input. A model for this experiment is considered in [15,16]. The perturbation to the conduction state temperature profile is assumed to take the form

$$
\Theta(X, Y, Z, t)
$$
$$
= \epsilon^{1/2}\,\mathrm{Re}\big\{z_+(t)f_+(X, Y, Z) + z_-(t)f_-(X, Y, Z)\big\}
$$
$$
+ \mathcal{O}(\epsilon),
$$

where $\epsilon \ll 1$, $f_\pm(-X, Y, Z) = \pm f_\pm(X, Y, Z)$. Here z_+ and z_- are the (complex) amplitudes of the first modes to lose stability which are respectively even and odd under the reflection $X \to -X$. In [15], evolution

equations for z_+ and z_- were derived using symmetry arguments, with the resulting equations describing a Hopf bifurcation with broken D_4 symmetry. The applicability of this model to the experiment is discussed further in [23]. As shown in [15,16], solutions of the evolution equations include bursts of very large dynamic range similar to those found in the experiments. The mechanism by which these bursts arise is discussed in detail in [17] and is summarized below.

In this Letter we generalize the model considered in [15,16] to include additive random forcing terms. Specifically, we consider the formal equations

$$\frac{dz_+}{dt} = \big(\lambda + \Delta\lambda + i(\omega + \Delta\omega)\big)z_+$$
$$+ A\big(|z_+|^2 + |z_-|^2\big)z_+ + B|z_+|^2 z_+$$
$$+ C\bar{z}_+ z_-^2 + \eta_1(t) + i\eta_2(t), \tag{1}$$

$$\frac{dz_-}{dt} = \big(\lambda - \Delta\lambda + i(\omega - \Delta\omega)\big)z_-$$
$$+ A\big(|z_+|^2 + |z_-|^2\big)z_- + B|z_-|^2 z_-$$
$$+ C\bar{z}_- z_+^2 + \eta_3(t) + i\eta_4(t), \tag{2}$$

where the η_i's represent real, independent Gaussian white noise random processes with the properties

$$\langle \eta_i(t)\rangle = 0, \qquad \langle \eta_i(t)\eta_j(t')\rangle = 2\mathcal{D}\delta(t-t')\delta_{ij},$$
$$i, j = 1, 2, 3, 4. \tag{3}$$

Here z_+, z_-, A, B, C are complex, and $\lambda, \Delta\lambda, \omega, \Delta\omega,$ $\mathcal{D}$ are real. The quantity $\Delta\omega$ measures the difference in frequency between the two modes at onset, and $\Delta\lambda$ measures the difference in their linear growth rates. The terms involving $\Delta\lambda$ and $\Delta\omega$ are called forced symmetry-breaking terms because they break the D_4 symmetry of the governing equations [16]. The new η_i terms represent unavoidable random effects in the experiment.

We first summarize results for the case that there is no noise, i.e., when $\mathcal{D} = 0$. New coordinates $(\rho, \theta, \phi, \psi)$ are defined according to

$$z_+ = \rho^{-1/2}\cos(\theta/2)e^{i(\phi+\psi)/2},$$
$$z_- = \rho^{-1/2}\sin(\theta/2)e^{i(-\phi+\psi)/2},$$

where without loss of generality $\theta \in [0, \pi]$, $\phi \in [-2\pi, 2\pi)$, and $\psi \in [0, 4\pi)$. Also introducing a new time τ defined by $d\tau/dt = 1/\rho$, Eqs. (1), (2) with

$\mathcal{D} = 0$ take the form

$$\frac{d\rho}{d\tau} = -\rho\big[2A_R + B_R\big(1 + \cos^2\theta\big) + C_R\sin^2\theta\cos 2\phi\big]$$
$$- 2(\lambda + \Delta\lambda\cos\theta)\rho^2, \tag{4}$$

$$\frac{d\theta}{d\tau} = \sin\theta\big[\cos\theta(-B_R + C_R\cos 2\phi) - C_I\sin 2\phi\big]$$
$$- 2\Delta\lambda\sin\theta\rho, \tag{5}$$

$$\frac{d\phi}{d\tau} = \cos\theta(B_I - C_I\cos 2\phi) - C_R\sin 2\phi + 2\Delta\omega\rho, \tag{6}$$

$$\frac{d\psi}{d\tau} = 2A_I + B_I + C_I\cos 2\phi + C_R\sin 2\phi\cos\theta$$
$$+ 2\omega\rho. \tag{7}$$

Here $A = A_R + iA_I$, etc. Let

$$r = \frac{1}{\rho} = |z_+|^2 + |z_-|^2$$

denote the amplitude of a solution. As discussed in [16,17], Eqs. (4)–(7) have an invariant subspace Σ at $\rho = 0$ (corresponding to infinite amplitude states) on which the equations are equivalent to those with $\Delta\lambda = \Delta\omega = 0$. Since the variable ψ decouples from the other variables, the dynamics on Σ are two-dimensional and hence simple to analyze [24]. Such an analysis (see [17]) allows us to conclude that, for this truncation, infinite amplitude periodic and quasiperiodic solutions exist. Bursts are associated with heteroclinic cycles involving such infinite amplitude states. Ref. [17] shows that for such cycles to form, it is necessary to have at least one subcritical and one supercritical solution branch bifurcating from the trivial state with $\Delta\lambda = \Delta\omega = 0$; also, the "angular stability" properties of the solutions must be correct. Ref. [17] also shows that despite their heteroclinic nature, the duration of the resulting bursts in the original time t is in fact *finite*, i.e., the excursion to and return from infinity occur in *finite* time. Of course, the infinite amplitude solutions and connections to them are of physical interest only insofar as they are responsible for the presence of nearby solutions which make visits to large but finite amplitude. This type of bursting behavior persists for $\mathcal{D} = 0$ even when higher-order terms in Eqs. (1), (2) are retained [17]. It should be emphasized that the noise is added on the original timescale t, not τ (see Eqs. (1), (2)).

3. Effect of noise on bursting behavior

We now describe the effect of noise on the bursting behavior reported in [15,16]. Coefficient values which give the appropriate sub- and supercriticality of traveling and standing wave branches in large aspect-ratio binary fluid convection systems are considered [16]:

$$A = 1 - 1.5i, \qquad B = -2.8 + 5i, \qquad C = 1 + i,$$

$$\omega = 1, \qquad \Delta\lambda = 0.03, \qquad \Delta\omega = 0.02.$$

For these coefficient values in the absence of noise, nonattracting, structurally stable heteroclinic cycles connecting infinite amplitude periodic orbits (hereafter, u_∞ solutions) and infinite amplitude quasiperiodic orbits (hereafter, qp_∞ solutions) exist over a range of λ values. These heteroclinic cycles are of Shil'nikov–Hopf type, and there are associated stable solutions which display bursting behavior [16,17].

For definiteness, consider the stable quasiperiodic solution which is present in the absence of noise for $\lambda = 0.1$ (see Fig. 1(a); in the notation of [17], this is a w_e^1 solution). The trajectory makes successive visits near *different* but symmetry-related u_∞ solutions given by $(\rho, \theta, \phi, \psi) = (0, \pi/2, m\pi, (2A_I + B_I + C_I)\tau \bmod 4\pi)$, $m = 0, \pm 1, \pm 2$. The u_∞ solutions are unstable within Σ, and the trajectory gets kicked toward a qp_∞ solution. The qp_∞ solutions are unstable in the ρ direction, so the trajectory returns to smaller amplitude (larger ρ). Physically, this solution corresponds to a *blinking state* for the convection system because successive bursts occur at opposite sides of the container [16]. Fig. 1(b) shows the corresponding results for $\mathcal{D} = 1 \times 10^{-7}$. Clearly, even this very small amount of noise can have a very large effect on the burst amplitudes. These and other numerical results were obtained using a stochastic second-order Runge–Kutta algorithm [25]. Unless otherwise indicated, the time step of integration is $\delta t = 1 \times 10^{-4}$.

The results shown in Fig. 1(b) may be qualitatively understood by recognizing that there will be a burst with larger amplitude if the noise kicks the trajectory closer to the stable manifold of a u_∞ solution, and a burst with smaller amplitude if the noise kicks it away. This is elucidated by ignoring the uncoupled variable ψ, linearizing Eqs. (4)–(6) about the u_∞ solutions, and defining coordinates (ρ, x, y) to give

the diagonal form

$$\frac{dx}{d\tau} = \lambda_u x, \qquad \frac{d\rho}{d\tau} = -\lambda_s \rho, \qquad \frac{dy}{d\tau} = -\lambda_{ss} y, \quad (8)$$

where $\lambda_u, \lambda_s, \lambda_{ss} > 0$. The stable manifold of the u_∞ solutions then approximately intersects a plane of sufficiently small, constant ρ along the line $x = 0$. For the parameters under consideration, $\lambda_u = 0.0682$, $\lambda_s = 0.2$, and $\lambda_{ss} = 5.868$, and Eq. (8) is obtained by using the coordinates approximately given by

$$\begin{pmatrix} \rho \\ x \\ y \end{pmatrix} = \begin{pmatrix} 1 & 0 & 0 \\ 0.269 & -0.730 & 0.706 \\ 0.00626 & 0.902 & 0.467 \end{pmatrix} \begin{pmatrix} \rho \\ \theta - \pi/2 \\ \phi - m\pi \end{pmatrix}.$$

Fig. 2(a) shows values at which the trajectory intersects the surface $\rho = 1$ with decreasing ρ for $\mathcal{D} = 1 \times 10^{-7}$. This is interpreted as showing how the noise affects the proximity of the trajectory to the stable manifold of the u_∞ solutions. The probability distribution function (pdf) of x values at the surface $\rho = 1$ is shown in Fig. 2(b). By definition, $p(x)\,dx$ is the probability that the x value at the surface $\rho = 1$ is between x and $x + dx$. This is fit reasonably well by the Gaussian distribution

$$p(x) = \frac{1}{\sqrt{2\pi\sigma_x^2}} \exp\left[-(x - \bar{x})^2 / (2\sigma_x^2)\right]. \tag{9}$$

Fig. 2(c) shows that the variances σ_x^2 of fitted Gaussians vary linearly with the noise strength $\mathcal{D}$. Over this range $\bar{x} \approx 0.200$, independent of $\mathcal{D}$. The noise strengths have been restricted to the range shown in the figure because for larger $\mathcal{D}$ the noise can kick the trajectory close enough to the stable manifold of a u_∞ solution that the long-time integration of Eqs. (1), (2) becomes numerically difficult.

Appendix A argues that it is reasonable to assume that the noise plays no significant role in the portion of the dynamics where the amplitude is large; the local deterministic dynamics near a u_∞ solution are then used to transform the pdf $p(x)$ at constant ρ to a pdf $p(\rho)$ at constant x for sufficiently small noise. Next we assume that in the trajectory's successive visits near u_∞ solutions, ρ always reaches its minimum value ρ_{min} at some *fixed* $x = x^*$. This is reasonable because at some x value the trajectory will have been kicked close to a qp_∞ solution which is *unstable* in the ρ direction, so the trajectory starts to evolve towards larger ρ (cf. Fig. 1). Then from (A.1), the pdfs for ρ_{min}
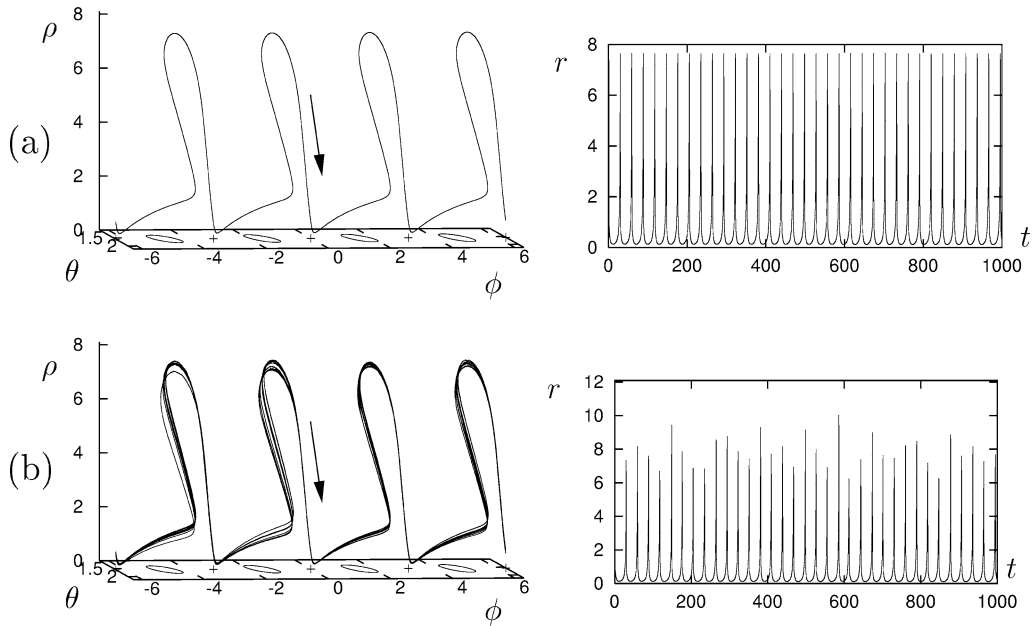
Fig. 1. Bursts for $\lambda = 0.1$ and (a) $\mathcal{D} = 0$, (b) $\mathcal{D} = 1 \times 10^{-7}$. Clearly, even a very small amount of noise can have a very large effect on the burst amplitudes. Fixed points (periodic orbits) in these projections correspond to periodic orbits (quasiperiodic orbits) for the full system. In this and later figures, the u_∞ solutions are denoted by $+$, and the qp_∞ solutions appear as periodic orbits at $\rho = 0$.
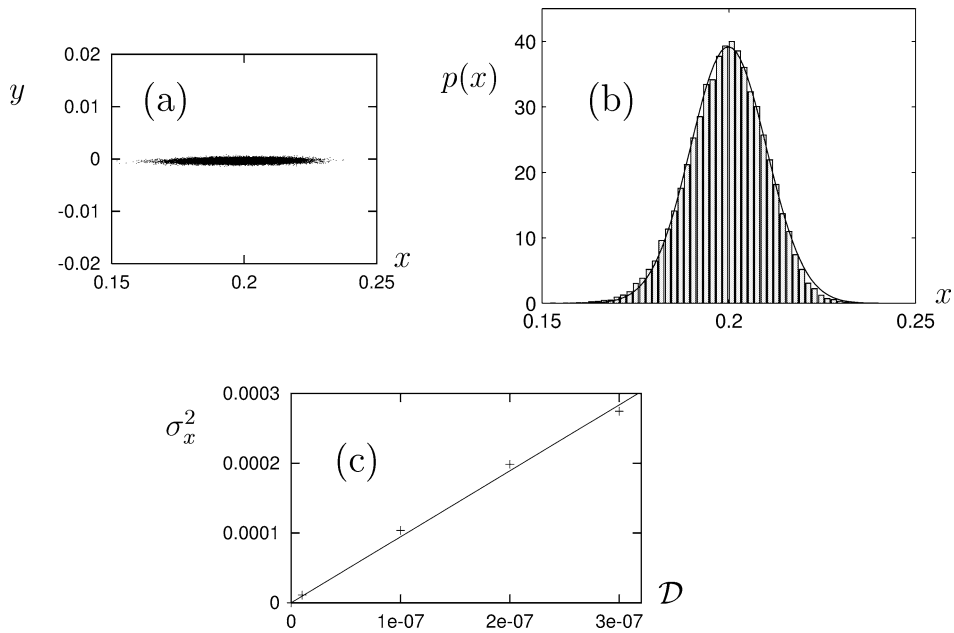

Fig. 2. (a) Values of (x, y) at which the trajectory intersects the surface $\rho = 1$ with decreasing ρ for $\mathcal{D} = 1 \times 10^{-7}$. The stable manifold of the u_∞ solutions intersects the surface $\rho = 1$ approximately along the line $x = 0$. (b) Probability distribution function $p(x)$ at the surface $\rho = 1$. The histogram is from a long-time integration of Eqs. (1), (2), and the solid line shows a fit to Eq. (9). (c) Variance σ_x^2 from fitting $p(x)$ to Eq. (9) for different noise strengths $\mathcal{D}$.
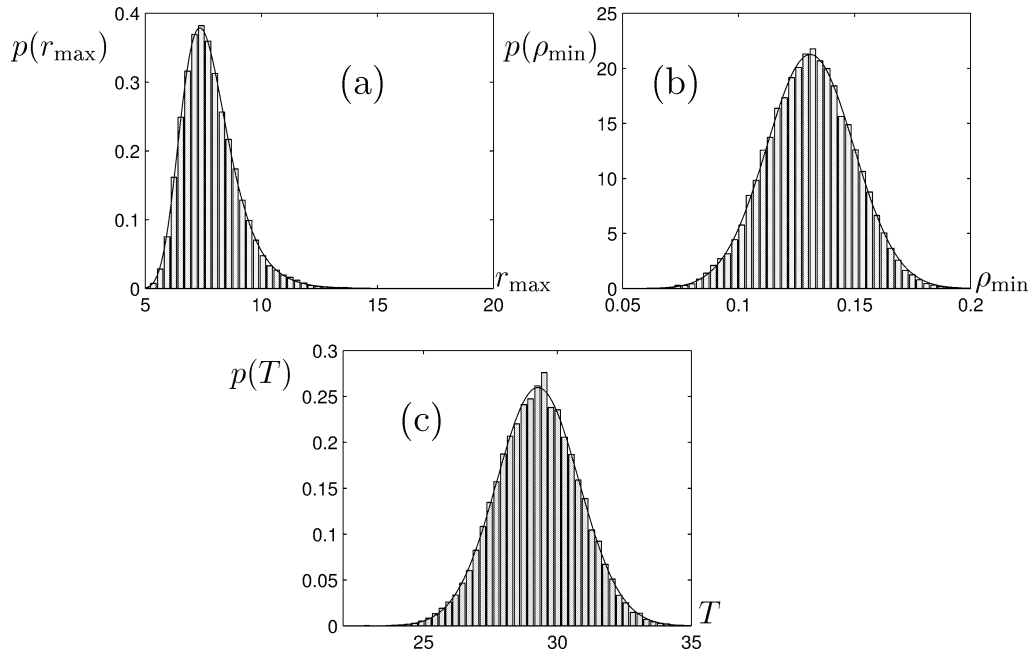
Fig. 3. Probability distribution functions for (a) r_{max}, (b) ρ_{min}, and (c) T for $\lambda = 0.1$, $\mathcal{D} = 1 \times 10^{-7}$. The histograms are from a long-time integration of Eqs. (1), (2), and the solid lines show fits given by Eqs. (10)–(12).

and $r_{max} = 1/\rho_{min}$ are

$$p(\rho_{min}) = \frac{1}{\sqrt{2\pi\sigma^2}}$$
$$\times \exp\left[-(\rho_{min} - \bar{\rho}_{min})^2/(2\sigma^2)\right], \qquad (10)$$

$$p(r_{max}) = \frac{1}{r_{max}^2 \sqrt{2\pi\sigma^2}}$$
$$\times \exp\left[-\left(\frac{1}{r_{max}} - \bar{\rho}_{min}\right)^2\Big/(2\sigma^2)\right]. \quad (11)$$

The $p(r_{max})$ distribution has a long $1/r_{max}^2$ tail for large r_{max}, indicating some probability of bursts having very large amplitudes. These functional forms for the pdf's are verified for $\mathcal{D} = 1 \times 10^{-7}$ in Figs. 3(a), (b). For the range of noise strengths considered, $\bar{\rho}_{min} \approx 0.131$ independent of $\mathcal{D}$; this is expected from (A.2) recalling that $\bar{x}$ was found to be independent of $\mathcal{D}$. The variance σ^2 of the fitted distributions is linear in the noise strength $\mathcal{D}$ (see Fig. 4(a)). This is also expected from (A.2) since $\bar{x}$ is independent of and σ_x^2 is linear in $\mathcal{D}$.

The statistics for the time T between successive bursts are shown in Fig. 3(c) for $\mathcal{D} = 1 \times 10^{-7}$. The pdf for T is fit very well by the Gaussian distribution

$$p(T) = \frac{1}{\sqrt{2\pi\sigma_T^2}} \exp\left[-\left(T - \bar{T}\right)^2\Big/(2\sigma_T^2)\right]. \qquad (12)$$

The variance σ_T^2 of the fitted distributions is linear in the noise strength $\mathcal{D}$ (see Fig. 4(b)), and $\bar{T} \approx 29.3$ is independent of $\mathcal{D}$. It is interesting to compare these results to the results of [8,9] which considered the effect of noise on attracting, structurally stable heteroclinic cycles connecting *finite* amplitude fixed points. It was found that the distribution of times between successive visits near the fixed points on the cycle was *not* Gaussian; instead, it has a long, exponential tail for large times. There is a fundamental reason for the difference between those results and the results presented here: because the heteroclinic cycles considered in [8,9] connect *finite* amplitude solutions, the trajectory spends most of its time in a small neighborhood these solutions. Indeed, this is what allowed a detailed analysis for the times between successive
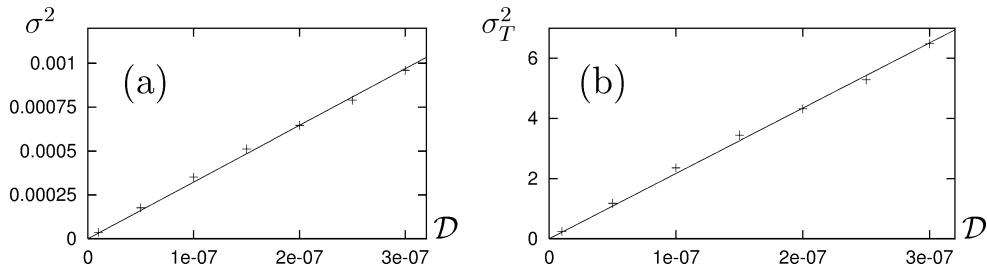
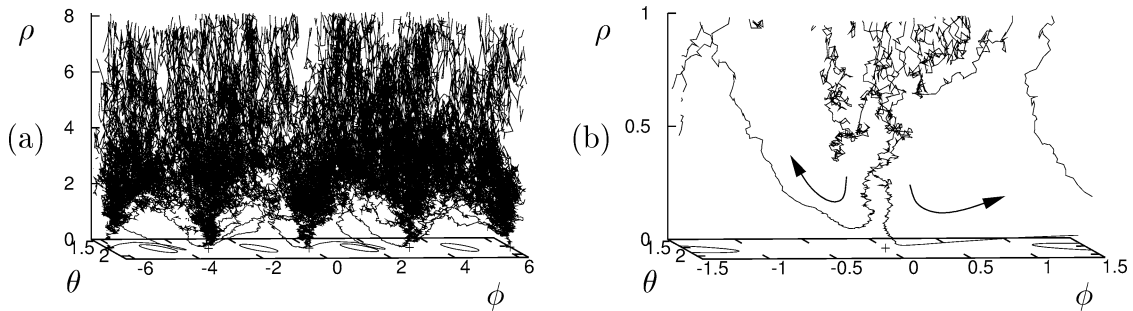Fig. 4. Linear dependence of the variances (a) σ^2, (b) σ_T^2 on the noise strength $\mathcal{D}$.

Fig. 5. (a), (b) Trajectory for $\lambda = 0.1$ and $\mathcal{D} = 0.01$. (b) shows the detail near the u_∞ solution at $(\rho, \theta, \phi) = (0, \pi/2, 0)$, and the arrows show the sense in which the trajectory is evolving.

visits near the fixed points to be done. On the other hand, the heteroclinic cycles considered in this Letter involve *infinite* amplitude solutions and are traced out in *finite* time [17]. More specifically, in the original time t defined by $dt/d\tau = \rho$, Eqs. (8) become

$$\frac{dx}{dt} = \frac{\lambda_u x}{\rho}, \qquad \frac{d\rho}{dt} = -\lambda_s.$$

Assuming the initial condition $(x_0, \rho) \in \Sigma_\rho$ at $t = 0$, these equations have the solution $x(t) = x_0(\rho^*/(\rho^* - \lambda_s t))^{\lambda_u/\lambda_s}$, $\rho(t) = -\lambda_s t + \rho^*$. The time to go from Σ_ρ to Σ_x is thus $t = (\rho^*/\lambda_s)(1 - (x_0/x^*)^{\lambda_s/\lambda_u})$. For the limit $x_0 \to 0$ (i.e., as the heteroclinic cycle is approached), $t \to \rho^*/\lambda_s$, a *finite* time. A similar argument shows that the trajectory also returns from infinity in finite time (cf. [17]). This is why the time series in Fig. 1(a) shows very rapid growth to and decay from large amplitude. We conclude that the time spent near solutions at infinity is not a dominant part of the total time between bursts. Thus, the results given in [8,9] are not relevant here. It is not possible to do detailed analytical work for the statistics of the

times between bursts without a more detailed understanding of how the trajectory behaves away from the u_∞ solutions. However, the model described in Appendix A gives some qualitative understanding, predicting a Gaussian distribution for the time between successive bursts with the average time between bursts independent of and the variance linear in $\mathcal{D}$. This is precisely what was found numerically.

Fig. 5 shows the projection of a numerical solution to Eqs. (1), (2) with the same parameter values as for the trajectories shown in Fig. 1, except with $\mathcal{D} = 0.01$. Unlike the result in Fig. 1(b) for much smaller noise strength, here the underlying stable quasiperiodic solution is not even recognizable. The arrows in Fig. 5(b) show that the trajectory can make a visit near a u_∞ solution and depart either to the "left" or to the "right". In the (ρ, x, y) coordinates introduced above (cf. Eq. (8)), the trajectory can intersect a surface of constant ρ for either positive or negative x values. Thus, sufficiently large noise can be responsible for the trajectory crossing the stable manifold of the u_∞ solutions. This leads to the possibil-
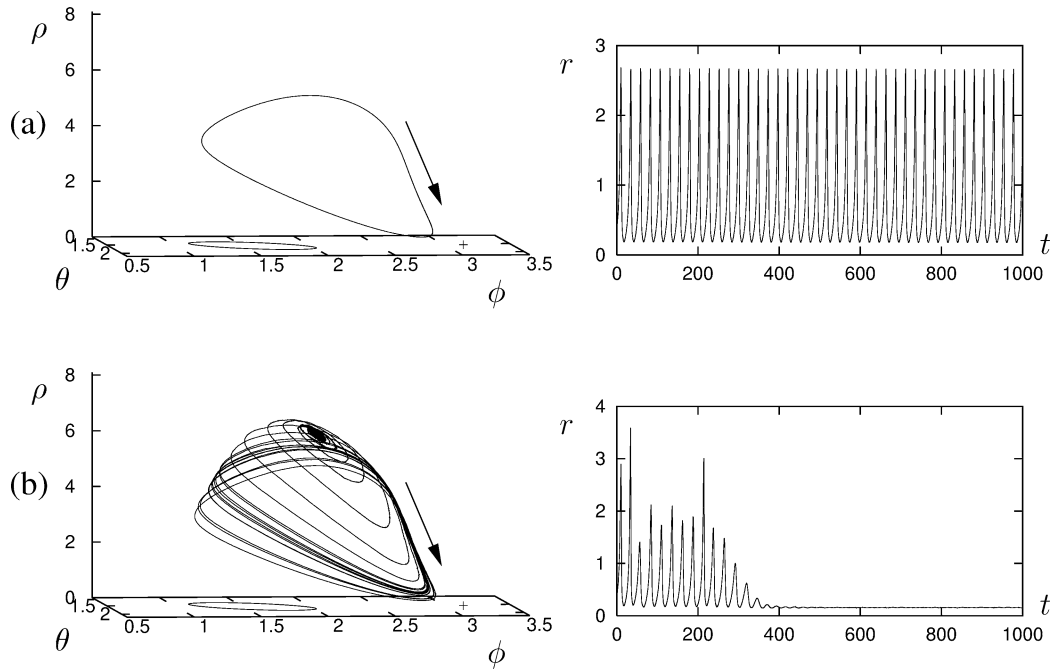
Fig. 6. Bursts for $\lambda = 0.1253$ and (a) $\mathcal{D} = 0$, (b) $\mathcal{D} = 1 \times 10^{-7}$. In (b), it is seen that the noise kicks the system out of the basin of attraction of the state shown in (a) and into the basin of attraction of a solution with constant $\rho = 1/r$.

ity that successive visits near infinity can either be to *different* or to the *same* u_∞ solutions. In the convection system, successive visits near the *same* u_∞ solution correspond to successive bursts occurring on the *same* side of the container [16]. Therefore, sufficiently large noise can affect the physical manifestation of the bursts by destroying purely blinking states. We note that such large noise will eventually kick the trajectory so close to a u_∞ solution that the accurate integration of Eqs. (1), (2) becomes very difficult.

Ref. [16] also identified a different type of stable quasiperiodic solution which is present in the absence of noise for $\lambda = 0.1253$ (in the notation of [17], this is a u/v^1 solution). The trajectory for this solution makes successive visits always near the *same* u_∞ solution (see Fig. 6(a)). Physically, this corresponds to a *winking state* for the convection system because successive bursts occur at the same side of the container [16]. This solution coexists with stable, finite amplitude periodic solutions at $(\rho, \theta, \phi) = (6.298, 1.753, 2.010 \pm m\pi)$, where m is an integer. Ref. [16] argues that these stable, finite amplitude periodic solutions are more likely

to be observed in experiments in which the Rayleigh number is ramped upwards, which helps to explain why winking states have apparently never been observed in binary fluid convection experiments. It is seen that even a very small amount of noise ($\mathcal{D} = 1 \times 10^{-7}$) can kick the system out of the basin of attraction of the winking state and into the basin of attraction of a stable periodic solution (see Fig. 6(b)). Thus, even if a winking state could be established in an experiment, it would be expected to be particularly sensitive to noise.

4. Noise-induced bursting

It will now be shown that related bursts may occur for Eqs. (1), (2) even in the absence of forced symmetry-breaking, that is, when noise is added to the normal form equations for the Hopf bifurcation with *exact* D_4 symmetry. Specifically, consider Eqs. (1), (2) with the same parameters as considered in the previous section ($A = 1 - 1.5i$, $B = -2.8 + 5i$, $C = 1 + i$,
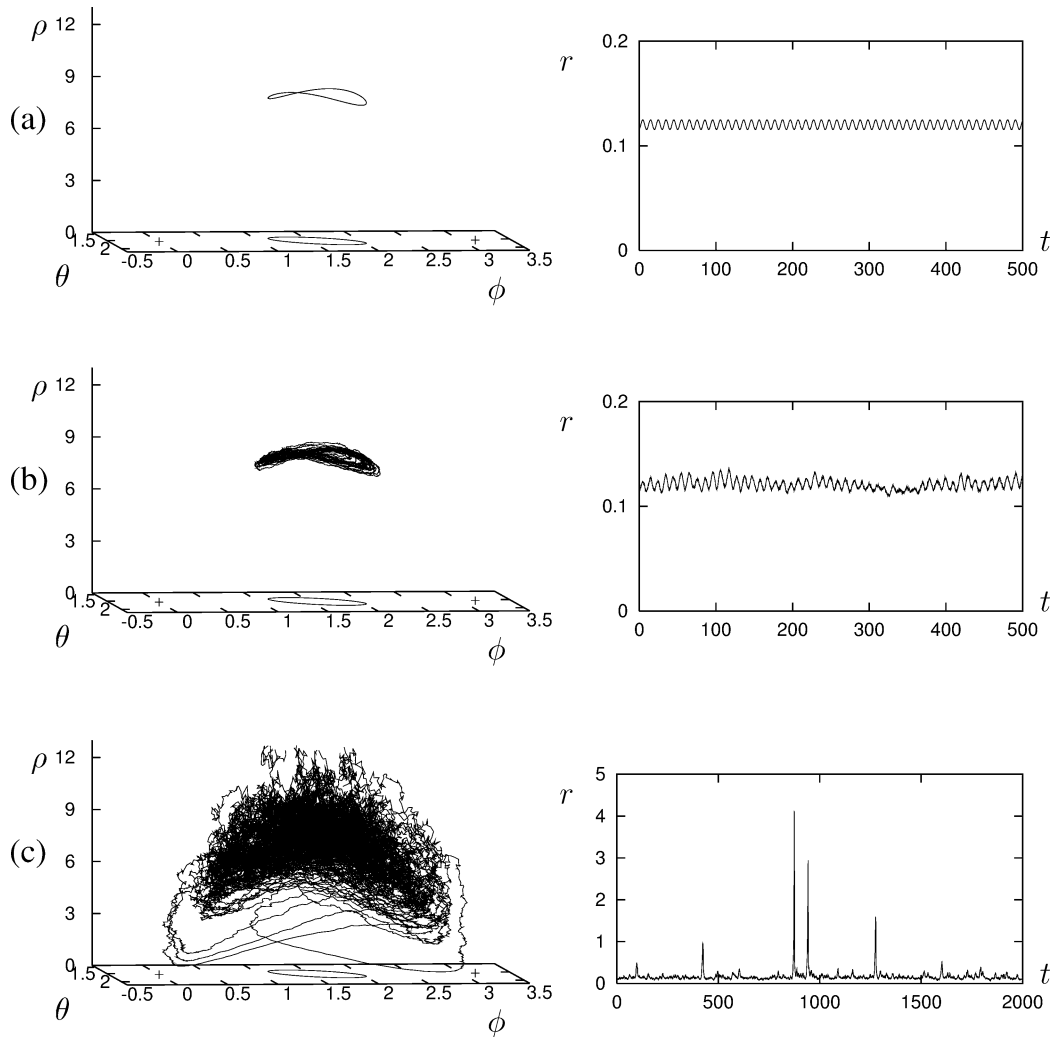
Fig. 7. Solutions for $\lambda = 0.1$ and (a) $\mathcal{D} = 0$, (b) $\mathcal{D} = 1 \times 10^{-6}$, (c) $\mathcal{D} = 1 \times 10^{-4}$ with $\Delta\lambda = \Delta\omega = 0$. Note the different scales for the time series plots.

$\omega = 1$), except with $\Delta\lambda = \Delta\omega = 0$. For these coefficient values in the absence of noise, a branch of unstable periodic solutions bifurcates subcritically from the trivial state, and two branches of unstable periodic orbits and one branch of globally attracting quasiperiodic solutions all bifurcate supercritically (see [24], also [16,17]). Infinite amplitude periodic and quasiperiodic solutions exist as counterparts of the finite amplitude solutions which bifurcate from the trivial state. In particular, u_∞ and qp_∞ solutions are the infinite amplitude counterparts of the periodic solu-

tions on the subcritical branch and quasiperiodic solutions on the supercritical branch, respectively [17]. If for some reason the trajectory comes close to the stable manifold of a u_∞ solution, it will make an excursion to a neighborhood of that solution, then get kicked toward a qp_∞ solution which returns it to smaller amplitude. However, since the finite amplitude quasiperiodic solutions are *globally* attracting, heteroclinic cycles involving infinite amplitude solutions cannot form, so such a burst is a transient phenomenon. A stable quasiperiodic solution is shown for
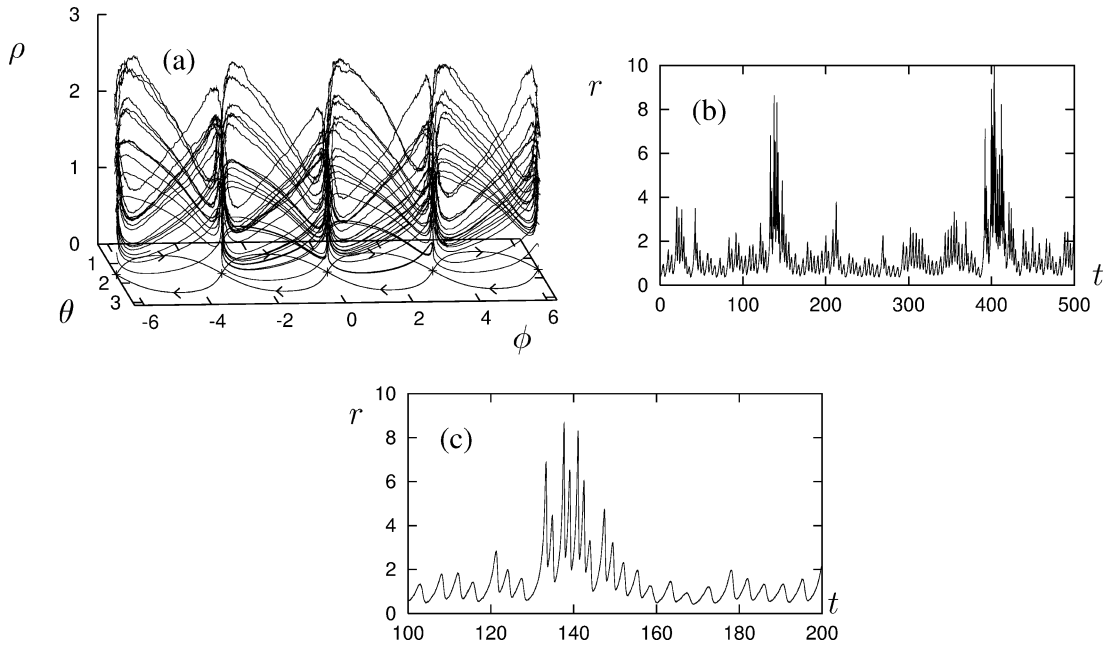
Fig. 8. (a) The attracting infinite amplitude heteroclinic cycle connecting u_∞ solutions at $\rho = 0$ and the solution for $\mathcal{D} = 1 \times 10^{-4}$. (b), (c) The time series for the solution with noise. Bursts occur in clumps of two types: faster with larger amplitudes (as for $130 \lesssim t \lesssim 150$) and slower with smaller amplitudes (as for $160 \lesssim t \lesssim 200$).

$\lambda = 0.1$, $\mathcal{D} = 0$ in Fig. 7(a). For small noise the trajectory remains near the quasiperiodic solution (see Fig. 7(b)). However, sufficiently large noise can repeatedly kick the system close to the stable manifold of a u_∞ solution, leading to bursts of very large dynamic range (see Fig. 7(c)). This is highly reminiscent of results for the effect of resonant temporal forcing on the Hopf bifurcation with D_4 symmetry [20]; there it was found that as the forcing amplitude increased, the attractor came closer to the stable manifolds of u_∞ solutions, leading to bursting behavior. We emphasize that bursting behavior cannot occur unless the parameters A, B, C give appropriate connections to and back from infinity [17]; for example, bursts cannot occur if A, B, C are such that there are no subcritical solution branches.

As a final demonstration of the effect of noise on a Hopf bifurcation with exact D_4 symmetry, we close by considering an *attracting* infinite amplitude heteroclinic cycle. Specifically, consider the parameters $A = 0.1 - 1.5i$, $B = -1 - 4i$, $C = 1 - 2i$, $\lambda = 0.1$, $\omega = 1$, $\Delta\lambda = \Delta\omega = 0$. Using the results of [24], it can

be shown that there are heteroclinic connections between u_∞ solutions *within* the $\rho = 0$ subspace. Linearizing Eqs. (4)–(6) about the u_∞ solutions shows that the eigenvalue corresponding to perturbations in the ρ direction is -0.2, while the eigenvalues corresponding to perturbations within the Σ subspace are -4.828 and 0.828. Since the first eigenvalue is negative and the sum of the latter two eigenvalues is also negative, the heteroclinic cycle connecting u_∞ is *attracting* (cf. [24]). Fig. 8 shows a numerically calculated trajectory for these parameter values and $\mathcal{D} = 1 \times 10^{-4}$; the time step of integration is $\delta t = 1 \times 10^{-5}$. Here noise causes bursts to occur in clumps of two types: faster with larger amplitudes, and slower with smaller amplitudes.

5. Conclusion

The effect of additive white noise on a model for large aspect-ratio binary fluid convection has been considered. Particular attention has been paid to the

effect of noise on bursting behavior present in the model. It was shown that even a very small amount of noise can have a very large effect on the amplitudes of successive bursts. This is because there will be a burst with larger amplitude if the noise kicks the system closer to the stable manifold of an infinite amplitude state, and a burst with smaller amplitude if the noise kicks it away. Numerical results and analytical arguments were given to understand the statistical properties of bursts in the presence of noise. It was also demonstrated that large enough noise can affect the physical manifestations of the bursts by destroying purely blinking and purely winking states. In fact, winking states are particularly sensitive to noise, which helps to explain why they have apparently never been observed in experiments. Finally, it was shown that related bursts can occur when noise is added to the normal form equations for the Hopf bifurcation with *exact* square symmetry. It is not immediately clear how to do more detailed analytical work on the effect of noise on the bursting behavior: there are no invariant sets near which the noisy trajectory spends most of its time; the behavior near such invariant sets is crucial to the analyses given in [1–3] and [8,9].

Reasoning similar to that given in [17] suggests that this type of bursting behavior can persist when higher terms in Eqs. (1), (2) are retained, even in the presence of noise. Bursts will then be associated with visits near large but *finite* amplitude solutions. This is important because it implies that bursts similar to those described in this Letter may be observed in real physical systems undergoing a Hopf bifurcation with exact or weakly broken D_4 symmetry; the (unphysical) infinite amplitude solutions are not necessary. There is also a possibility that in appropriate cases the noise could be more important than higher-order terms so their exact nature would be irrelevant.

Other physical systems for which the results presented in the Letter might be relevant because their evolution equations are related to the Hopf bifurcation with D_4 symmetry include any system in a square domain undergoing an oscillatory instability [26] or displaying oscillatory patterns which are periodic on a square lattice [27], electrohydrodynamic convection in liquid crystals [28], lasers [29], spring-supported fluid-conveying tubes [30], the Faraday system in a square or nearly-square container [31], and dynamo theories of magnetic field generation in the Sun [19,32].

Acknowledgements

Appendix A

We first show how to understand the statistical properties of the amplitudes of the bursts in terms of $p(x)$ as given by (9). In the following, we ignore the strongly contracting y direction. Define

$$\Sigma_\rho = \left\{ (x, \rho) \,\big|\, \rho = \rho^* \right\} \quad \text{and}$$
$$\Sigma_x = \left\{ (x, \rho) \,\big|\, x = x^* \right\},$$

and consider how the pdf $p(x)$ at Σ_ρ evolves into a pdf $p(\rho)$ at Σ_x (see Fig. 9). When the amplitude r becomes large (i.e., when ρ becomes small), the noise terms in Eqs. (1), (2) are overwhelmed by the cubic deterministic terms. Therefore, provided ρ^* is sufficiently small, we can ignore the noise over the part of the trajectory shown in Fig. 9 and approximate the vector field by Eq. (8). The point $(x_0, \rho^*) \in \Sigma_\rho$ is mapped into $(x^*, f(x_0)) \in \Sigma_x$ under the flow, where $f(x) \equiv \rho^*(x/x^*)^{\lambda_s/\lambda_u}$. Given $p(x)$, the pdf $p(\rho)$ is obtained using $|p(x)\,dx| = |p(\rho)\,d\rho|$, with $\rho = f(x)$. For sufficiently small noise we can take $f(x) \approx f(\bar{x}) + f'(\bar{x})(x - \bar{x})$, where $\bar{x}$ is the average value of x at Σ_ρ. (For larger noise strength, it may be necessary to use the exact expression for $f(x)$ because $p(x)$ will be a broader distribution.) Using (9) as the
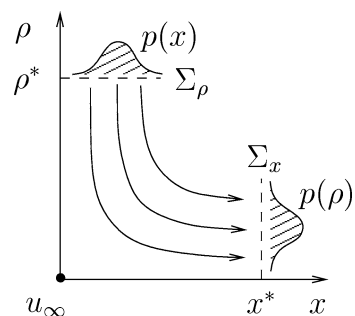

Fig. 9. Setup for determining how the pdf of x values at constant $\rho = \rho^*$ evolves into a pdf of ρ values at constant $x = x^*$.

pdf for x at Σ_ρ, the pdf for ρ at Σ_x is then

$$p(\rho) = \frac{1}{\sqrt{2\pi\sigma^2}} \exp\left[-(\rho - \bar{\rho})^2 / (2\sigma^2)\right], \qquad \text{(A.1)}$$

$$\sigma^2 = \left(f'(\bar{x})\right)^2 \sigma_x^2, \qquad \bar{\rho} = f(\bar{x}). \qquad \text{(A.2)}$$

We next give a model to help understand the statistics for the time between bursts. Consider

$$\frac{d\xi}{dt} = v + \eta(t), \qquad \text{(A.3)}$$

where v is constant, and η is a Gaussian white noise random process with $\langle\eta(t)\rangle = 0$ and $\langle\eta(t)\eta(t')\rangle = 2\mathcal{D}\delta(t - t')$. If $\xi = \xi_0 = 0$ at $t = 0$, the conditional probability distribution function $P(\xi, t|\xi_0)$ for solutions of Eq. (A.3) obeys the Fokker–Planck equation

$$\partial_t P = -\partial_\xi(vP) + \mathcal{D}\partial_{\xi\xi}P,$$

$$P = \delta(\xi) \quad \text{for } t = 0.$$

This has solution

$$P(\xi, t|\xi_0 = 0) = \frac{1}{\sqrt{4\pi\mathcal{D}t}} \exp\left(-(\xi - vt)^2 / (4\mathcal{D}t)\right),$$

i.e., a Gaussian centered at $\xi = vt$ and with variance $2\mathcal{D}t$. The average time to reach a *fixed* value $\xi = \xi^*$ is then $\bar{T} \equiv \xi^*/v$, and the pdf for ξ at this time is $p(\xi) \equiv P(\xi, \bar{T}|\xi_0 = 0)$. We can re-express this in terms of a pdf for the time T at which $\xi = \xi^*$ by using the deterministic approximation $T \approx \bar{T} - (\xi - \xi^*)/v$. Then, using $|p(\xi)\,d\xi| = |p(T)\,dT|$, we obtain

$$p(T) = \frac{v}{\sqrt{4\pi\mathcal{D}\bar{T}}} \exp\left(-v^2(T - \bar{T})^2 / (4\mathcal{D}\bar{T})\right).$$

We make a connection to the distribution of times between successive bursts by thinking of ξ as an arclength coordinate along a trajectory for Eqs. (1), (2), keeping in mind that the trajectory does not spend a dominant part of its time in a neighborhood of the u_∞ and qp_∞ solutions. Assuming that the arclength traced out between successive bursts is roughly constant as will be the case for sufficiently small noise, (A.3) thus predicts a Gaussian distribution for the time between successive bursts with the average time between bursts independent of and the variance linear in $\mathcal{D}$.

References

[1] D.W. Hughes, M.R.E. Proctor, Physica D 46 (1990) 163.
[2] G.D. Lythe, M.R.E. Proctor, Phys. Rev. E 47 (1993) 3122.
[3] R. Kuske, G. Papanicolaou, Physica D 120 (1998) 255.
[4] M. Georgiou, T. Erneux, Phys. Rev. A 45 (1992) 6636.
[5] G.D. Lythe, Nuovo Cimento D 17 (1995) 855.
[6] E. Stone, D. Armbruster, Chaos 9 (1999) 499.
[7] F.H. Busse, K.E. Heikes, Science 208 (1980) 173.
[8] E. Stone, P. Holmes, Physica D 37 (1989) 20.
[9] E. Stone, P. Holmes, SIAM J. Appl. Math 50 (1990) 726.
[10] R. Benzi, S. Sutera, A. Vulpiani, J. Phys. A 14 (1981) L453.
[11] R. Benzi, G. Parisi, A. Sutera, A. Vulpiani, Tellus 34 (1982) 10.
[12] R. Benzi, G. Parisi, A. Sutera, A. Vulpiani, SIAM J. Appl. Math. 43 (1983) 565.
[13] L. Gammaitoni, P. Hänggi, P. Jung, F. Marchesoni, Rev. Mod. Phys. 70 (1998) 223.
[14] K. Wiesenfeld, F. Jaramillo, Chaos 8 (1998) 539.
[15] A.S. Landsberg, E. Knobloch, Phys. Rev. E 53 (1996) 3579.
[16] J. Moehlis, E. Knobloch, Phys. Rev. Lett. 80 (1998) 5329.
[17] J. Moehlis, E. Knobloch, Physica D 135 (2000) 263.
[18] T.S. Sullivan, G. Ahlers, Phys. Rev. A 38 (1988) 3143.
[19] E. Knobloch, A.S. Landsberg, Mon. Not. R. Astron. Soc. 278 (1996) 294.
[20] J. Moehlis, E. Knobloch, Physica D, to appear.
[21] E. Knobloch, J. Moehlis, in: M. Golubitsky, D. Luss, S.H. Strogatz (Eds.), Pattern Formation in Continuous and Coupled Systems: A Survey Volume, Springer, New York, 1999, pp. 157–174.
[22] E. Knobloch, J. Moehlis, in: L. Debnath, D. Riahi (Eds.), Nonlinear Instability, Chaos, and Turbulence, Vol. II, Computational Mechanics Publications, Southampton, 2000, pp. 237–287.
[23] O. Batiste, I. Mercader, M. Net, E. Knobloch, Phys. Rev. E 59 (1999) 6730.
[24] J.W. Swift, Nonlinearity 1 (1988) 333.
[25] R.L. Honeycutt, Phys. Rev. A 45 (1992) 600.
[26] P. Ashwin, Z. Mei, Nonlinearity 8 (1995) 715.
[27] M. Silber, E. Knobloch, Nonlinearity 4 (1991) 1063.
[28] H. Riecke, M. Silber, L. Kramer, Phys. Rev. E 49 (1994) 4100.
[29] Q. Feng, J.V. Moloney, A.C. Newell, Phys. Rev. A 50 (1994) R3601.
[30] A. Steindl, H. Troger, Nonlinear Dynam. 8 (1995) 161.
[31] F. Simonelli, J.P. Gollub, J. Fluid Mech. 199 (1989) 471.
[32] E. Knobloch, S.M. Tobias, N.O. Weiss, Mon. Not. R. Astron. Soc. 297 (1998) 1123.